HHS Public Access

Author manuscript

Clin Cancer Res. Author manuscript; available in PMC 2016 April 09.

Published in final edited form as:

Clin Cancer Res. 2013 October 15; 19(20): 5711–5721. doi:10.1158/1078-0432.CCR-12-1015.

Preclinical Efficacy of the Anti-Hepatocyte Growth Factor Antibody Ficlatuzumab in a Mouse Brain Orthotopic Glioma Model Evaluated by Bioluminescence, PET, and MRI

Erik S. Mittra[1], **Hua Fan-Minogue**[1,2], **Frank I. Lin**[1], **Jason Karamchandani**[3], **Venkataraman Sriram**[4], **May Han**[5], and **Sanjiv S. Gambhir**[1,6]

[1]Molecular Imaging Program, Department of Radiology

[2]System Medicine, Department of Pediatrics

[3]Division of Neuropathology, Department of Pathology

[4]Merck Research Laboratories, Palo Alto, California

[5]AVEO Pharmaceuticals Inc., Cambridge, Massachusettes

[6]Bio-X Program, Department of Bioengineering, Department of Materials Science & Engineering, Stanford University, Stanford

Abstract

Purpose—Ficlatuzumab is a novel therapeutic agent targeting the hepatocyte growth factor (HGF)/c-MET pathway. We summarize extensive preclinical work using this agent in a mouse brain orthotopic model of glioblastoma.

Experimental Design—Sequential experiments were done using eight- to nine-week-old nude mice injected with 3×10^5 U87 MG (glioblastoma) cells into the brain. Evaluation of ficlatuzumab dose response for this brain tumor model and comparison of its response to ficlatuzumab and to temozolamide were conducted first. Subsequently, various small-animal imaging modalities,

Corresponding Author: Sanjiv S. Gambhir, Department of Radiology, Molecular Imaging Program at Stanford (MIPS), Canary Center at Stanford for Cancer Early Detection, Nuclear Medicine, Stanford University School of Medicine, James H. Clark Center, 318 Campus Drive, E153, Stanford, CA 94305. Phone: 650-725-2309; Fax: 650-724-4948; sgambhir@stanford.edu.

Note: Supplementary data for this article are available at Clinical Cancer Research Online (http://clincancerres.aacrjournals.org/).

Disclosure of Potential Conflicts of Interest

M. Han has ownership interest (including patents) in AVEO Pharmaceuticals, Inc. No potential conflicts of interest were disclosed by the other authors.

Authors' Contributions

Conception and design: E.S. Mittra, F.I. Lin, V. Sriram, M. Han, S.S. Gambhir

Development of methodology: E.S. Mittra, H. Fan-Minogue, F.I. Lin, V. Sriram, S.S. Gambhir

Acquisition of data (provided animals, acquired and managed patients, provided facilities, etc.): E.S. Mittra, H. Fan-Minogue, F.I. Lin, J. Karamchandani, V. Sriram

Analysis and interpretation of data (e.g., statistical analysis, biostatistics, computational analysis): E.S. Mittra, H. Fan-Minogue, J. Karamchandani, S.S. Gambhir

Writing, review, and/or revision of the manuscript: E.S. Mittra, H. Fan-Minogue, F.I. Lin, J. Karamchandani, S.S. Gambhir

Administrative, technical, or material support (i.e., reporting or organizing data, constructing databases): E.S. Mittra, S.S. Gambhir

Study supervision: E.S. Mittra, S.S. Gambhir

Performed portions of the study reported in the manuscript: E.S. Mittra, F.I. Lin

including bioluminescence imaging (BLI), positron emission tomography (PET), and MRI, were used with a U87 MG-Luc 2 stable cell line, with and without the use of ficlatuzumab, to evaluate the ability to non-invasively assess tumor growth and response to therapy. ANOVA was conducted to evaluate for significant differences in the response.

Results—There was a survival benefit with ficlatuzumab alone or in combination with temozolamide. BLI was more sensitive than PET in detecting tumor cells. Fluoro-D-thymidine (FLT) PET provided a better signal-to-background ratio than 2[^{18}F]fluoro-2-deoxy-D-glucose (FDG) PET. In addition, both BLI and FLT PET showed significant changes over time in the control group as well as with response to therapy. MRI does not disclose any time-dependent change. Also, the MRI results showed a temporal delay in comparison to the BLI and FLT PET findings, showing similar results one drug cycle later.

Conclusions—Targeting the HGF/c-MET pathway with the novel agent ficlatuzumab appears promising for the treatment of glioblastoma. Various clinically applicable imaging modalities including FLT, PET, and MRI provide reliable ways of assessing tumor growth and response to therapy. Given the clinical applicability of these findings, future studies on patients with glioblastoma may be appropriate.

Introduction

Primary brain tumors are rare, with an incidence of 6.4 per 100,000 men and women per year in the United States, and a male-to-female ratio of 6:4 (1). Gliomas account for 30% to 40% of all intracranial tumors, of which approximately half are glioblastomas in adults, with a peak incidence between the ages of 40 and 65 years (2). Although gliomas are rare, they are medically important because of poor clinical outcomes. As such, there is considerable ongoing research on novel therapeutics for glioblastoma.

One such agent is the anti-hepatocyte growth factor (HGF) antibody ficlatuzumab (AV-299; SCH 900105). Developed by Aveo Pharmaceuticals, it is a potent anti-HGF/c-MET antibody currently in phase II trials. The HGF/ c-MET pathway is thought to play an important role in regulating tumor growth, invasion, and metastasis. Deregulation of this pathway has been implicated in many tumors, including bladder, lung, breast, gastric, ovarian, prostate, colorectal, head and neck, certain sarcomas and several other solid tumors as well as hematologic malignancies. Ficlatuzumab has high affinity on the ligand HGF, thereby blocking the c-MET pathway. Initial clinical data of ficlatuzumab indicate a favorable tolerability profile, good combinability with other chemotherapeutic agents, and no dose-limiting toxicities noted (3, 4).

Translational Relevance

Human gliomas have a poor prognosis and therapeutic options are limited. Ficlatuzumab is a novel therapeutic agent against the hepatocyte growth factor (HGF)/ c-MET pathway. Extensive preclinical work for ficlatuzumab using a mouse brain orthotopic model of glioblastoma is summarized here. This includes evaluation of dose response, comparison to the current standard of care, temozolomide, and ultimately noninvasive assessment of tumor response using a combination of bioluminescence imaging (BLI), small-animal

positron emission tomography (PET), and small-animal MRI. Ficlatuzumab provides a survival benefit both alone and in conjunction with temozolomide. PET with fluoro-D-thymidine (FLT) provided a distinct advantage in this model over 2[^{18}F]fluoro-2-deoxy-D-glucose (FDG). And, while not as sensitive as BLI, both FLT PET and MRI were able to assess response to therapy noninvasively. MRI may provide complimentary information to BLI and FLT PET. As such, combined (MRI–PET fusion) imaging may have a role.

On the basis of this prior work, the purpose of this experiment is to evaluate via molecular imaging the efficacy of ficlatuzumab in an orthotopic glioblastoma model in mice. Through a series of preclinical experiments, we evaluate the dose response of ficlatuzumab, efficacy of ficlatuzumab alone versus in conjunction with the standard-of-care chemotherapy temozolomide, and then assess tumor response *in vivo* using a combination of bioluminescence imaging (BLI), small-animal positron emission tomography (PET), and small-animal MRI.

Materials and Methods

Nonimaging studies on dose titration of ficlatuzumab and combination versus monotherapy with temozolomide

Cell culture—Human U87 malignant glioma (MG) cells were obtained from The American Type Culture Collection (ATCC; HTB-14) and maintained at low passage number. The cells were cultured in Dulbecco's Modified Eagle's Medium (DMEM) supplemented with 10% FBS and maintained at 37°C in an atmosphere containing 5% CO_2 and 95% air. Cells for implantation were used within 5 subculture periods after thawing from liquid nitrogen stock. Only log-phase culture of cells at 70% to 80% confluency and more than 90% viability were used for implantation. On the day of surgery, U87 MG cells were collected by trypsinization and resuspended in PBS to obtain 3×10^5 cells in 2 μL for injection purposes. U87 cells secrete about 10 to 15 ng/mL of HGF in the culture medium after 24 to 48 hours of culture. They express relatively low levels of c-Met as detected by fluorescence-activated cells sorting (FACS) analysis and Western blotting.

Tumor implantation and experimental design—A total of 80 mice were investigated in this nonimaging portion of the experiment. The mice were housed in a microventilated caging system with controlled temperature (68°F ± 2°F), humidity (30%–70%), room ventilation (10–15 air changes per hour), and a lighting cycle of 12-hour light/dark. Five mice were housed per autoclaved cage and had free access to standard irradiated research rodent diet (Harlan Teklad) and water during the experimental period. All mice were treated in accordance with the Institutional Animal Use and Care Committee (Merck Research Laboratories and Stanford University) guidelines as set forth in OLAW Public Health Service Policy on Humane Care and Use of Laboratory Animals and the ILAR Guide for the Care and Use of Laboratory Animals. Eight- to 9-week-old female nude mice (NuNu, Charles River Laboratories or NCr-Nude, Taconic) were anesthetized using 2% isoflurane and positioned in a Benchmark (Leica) stereotactic instrument.

The top of the animal's head was cleaned with 70% ethanol and betadine. Ophthalmic ointment was applied, a linear skin incision was made over the bregma, and 3% hydrogen peroxide was applied to the periosteum with a cotton swab. A 27-gauge needle was then used to drill a burrhole into the skull 0.5-mm anterior and 2-mm lateral to the bregma. A 10-μL gas-tight syringe (Hamilton) was then used to inject 2 μL of the U87 MG-Luc2 cell suspension (3×10^5 cells in PBS) in the striatum at a depth of 3 mm from the dural surface. The injection was slowly done over 10 minutes. The burrhole was occluded with glue to prevent leakage of cerebrospinal fluid and the skin was closed with surgical clips. Before being allowed to awaken from anesthesia, the mice also received a subcutaneous injection of 0.1 mL of a 1:10 dilution of 0.3-mg/mL buprenorphine as additional analgesia. The surgical clips were removed at the time of baseline imaging 1 to 2 weeks later.

To evaluate the dose titration of ficlatuzumab, 10 to 14 days postinoculation, the mice with tumors were randomized into 4 groups of 10 mice each. The 4 groups included a control group and 3 groups of increasing ficlatuzumab doses (5, 10, or 20 mg/kg per administration). The drug was given intraperitoneally twice per week, and survival duration was recorded as the endpoint. Mice were monitored periodically for clinical signs of tumor burden and body weights tracked using StudyDirector (Studylog Systems, Inc.) software program. Mice were sacrificed when they exhibited signs of being moribund and/or more than 20% body weight loss.

To evaluate the relative efficacy of ficlatuzumab to temozolomide, again 10 to 14 days postinoculation, the mice with tumors were randomized into 4 groups of 10 mice each. In this case, the 4 groups included those treated with human IgG control (10 mg/kg), ficlatuzumab alone (10 mg/kg), temozolomide alone (5 mg/kg), or the combination of ficlatuzumab plus temozolomide. Ficlatuzumab was given intraperitoneally twice per week, whereas temozolomide was given intraperitoneally for 5 consecutive days per 28-day treatment cycle. Both were continued for 120 days post-tumor implantation, and survival duration was again the endpoint. As above, mice were monitored periodically for clinical signs of tumor burden and sacrificed when they exhibited signs of being moribund and/or more than 20% body weight loss.

In vivo imaging studies to evaluate the tumor response to ficlatuzumab

The next phase of the study was to evaluate the response of glioblastoma tumors to ficlatuzumab *in vivo* using a combination of small-animal imaging modalities. The goal was to predict response to therapy less invasively and sooner than using survival as an endpoint. To achieve this goal, again several related but distinct experiments were done sequentially.

The first imaging modality to be evaluated was BLI. A U87 MG-Luc2 cell line was prepared. U87 MG-Luc2 is a luciferase-expressing cell line which was stably transfected with firefly luciferase gene (*Luc2*) and custom made for Merck Research Laboratories by Caliper Life Sciences. The cell line was established by transducing lentivirus-containing luciferase 2 gene (pGL4-Luc2; Promega) under the control of human ubiquitin C promoter. A clone that had stable luciferase expression for 4 weeks in the absence of selection pressure was selected and used in all experiments.

The second imaging modality to be evaluated was small-animal PET. In this case, an initial study was conducted to evaluate the relative use of 2[^{18}F]fluoro-2-deoxy-D-glucose (FDG) versus fluoro-D-thymidine (FLT) PET to assess tumor size and function using BLI as standard. For all these experiments, the cell culture and tumor implantation process was identical to that described previously for the non-imaging studies. To evaluate the relative use of FDG versus FLT PET, 1 week after tumor implantation, BLI was used to divide the mice into 2 groups of mice, selected to have similar BLI signal. The first (FDG group) had 7 mice, whereas the second (FLT group) had 8 mice. Starting 1 week after tumor implantation, weekly whole-body FDG or FLT small-animal PET scans, and BLI imaging, were done on these mice for a total of 5 weeks, for a total of 35 FDG PET and 40 FLT PET measurements. As before, mice were monitored periodically for clinical signs of tumor burden and sacrificed when they exhibited signs of being moribund and/or more than 20% body weight loss.

In the final study, 24 mice were used to evaluate the relative ability of BLI, small-animal PET, and micro-MRI to assess *in vivo* tumor response to ficlatuzumab. In this final experiment, 1 week after tumor implantation, the animals were separated into 3 groups again based on the BLI signal to ensure that each group had mice with similar starting tumor burden. The first, control group ($n = 8$) was given no drug injections. The second, low-dose group [$n = 7$ (1 mouse died during baseline imaging)] was given 3-mg/kg ficlatuzumab intraperitoneally every 3 days for a total of 3 doses. This dose was chosen in an attempt to give a suboptimal dose, as the prior studies showed no significant differences between the 5 and 10 mg/kg doses. The third, high-dose group ($n = 8$) was given 10 mg/kg ficlatuzumab intraperitoneally using the same schedule. The baseline imaging for each group of mice was started 16 days posttumor implantation for the control group and 19 days post-tumor implantation for the other 2 groups (overall average: 18 ± 1.7 days). The first drug dose was given the day following baseline imaging. The follow-up imaging time point was 2 days after each drug injection. All imaging, included bioluminescence, small-animal PET, and small-animal MRI, were done on the same day. The details of these modalities are given next.

In total, then, 80 mice were investigated for the nonimaging experiments and 38 mice were investigated for the imaging experiments.

Imaging details

Bioluminescence imaging—Each mouse was injected intraperitoneally with 0.1 mL of the substrate D-luciferin. Afterward, the mice were allowed to roam freely in their cages for approximately 1 minute, whereas the substrate was absorbed, circulated, and metabolized. Groups of up to 5 mice at a time were then anaesthetized using 2% isoflurane and placed in an optical imaging system (IVIS 200 Series, Xenogen), at approximately 2 minutes after D-luciferin injection. The specific imaging parameters (field of view, acquisition time, F-stop) were adjusted to optimize the signal (i.e., capture the largest signal allowable without saturating the image). These parameters were adjusted per scan as each group of mice had constantly differing signals on any given imaging day. Scanning was continued until the peak signal was captured. This occurred somewhere between 3 and 12 minutes after

injection of D-luciferin. After scanning, the mice were weighed on a standard laboratory scale and then allowed to recover in their cage.

Small-animal PET—Each mouse was sequentially anesthetized using 2% isoflurane and immediately injected intraperitoneally with 200 ± 20 μCi of the specified radio-pharmaceutical (either FDG or FLT). The mice were kept anesthetized for 60 minutes, whereas the radiopharmaceutical circulated, localized in tissue, and cleared to minimize nonspecific uptake in the skeletal muscle (including, in particular, ocular muscles) and brain. The mice were then placed individually (1st experiment) or in groups of 4 (2nd experiment) in a small-animal PET scanner (Concorde Microsystems MicroPET rodent R4 Scanner, Siemens Medical Systems). A 10-minute (1st experiment) or 15 minute (2nd experiment) static emission scan was then obtained and reconstructed (in 3 dimensions) using an iterative algorithm (Ordered Subset Expectation Maximization, OSEM). Attenuation and partial volume corrections were not conducted. After scanning, the mice were returned to their cage and allowed to recover.

Small-animal MRI—Each mouse was sequentially anesthetized using 2% isoflurane and placed supine in a specially designed stage with the top of its head centered in a small, circular MRI coil. The stage was then placed within the small-animal MRI system (Magnex/Varian self-shielded 30 cm bore 7 Tesla magnet with a Research Resonance Instruments 9 cm bore gradient insert and the GE HealthCare “Micro”-Signa software environment). A 15-second localizer scan was conducted first followed by a pre-scan to allow for manual gradient shimming. Then, a T2-weighted fast spin echo (FSE) sequence was obtained from the top of the head to the skull base. No contrast agents were given. This scan was approximately 5 minutes long for 30 slices and had an isotropic resolution of 20 μm. The mouse was then removed from the scanner and allowed to recover in its cage.

Image analysis—The bioluminescence images were analyzed using built-in software on the Xenogen IVIS system. Two-dimensional regions of interest (ROI) were manually drawn (by authors E.S. Mittra or H. Fan-Minogue) over the head and used to measure photon flux per area ($p/s/cm^2/sr$). The ROI size was not fixed but rather adjusted per animal to just encompass the entire region of photon flux.

The small-animal PET data were analyzed using image analysis software developed in-house in the Gambhir lab using Amide’s a Medical Imaging Data Examiner (AMIDE, http://amide.sourceforge.net/). Three-dimensional ROI were drawn (by E.S. Mittra) to measure mean percent injected dose per gram (%ID/g). The ROIs were drawn over the brain tumor itself as well as in the contralateral region of the brain to assess background activity.

The small-animal MRI data were analyzed using the commercially available DICOM image viewer OsiriX (http://www.osirix-viewer.com/). Lengths were measured (by E.S. Mittra) in 3 dimensions, including 2 in the transaxial plane (long and short axis), as well as along the craniocaudal direction.

Pathology

At the conclusion of the experiment, all mice were sacrificed using CO_2 gas inhalation. Three mice from each group had their whole brain extracted and placed intact into 10% formalin. These brain samples were then embedded in paraffin and 5-μm cross sections were stained with hematoxylin and eosin (H&E). Immunohistochemistry for Ki-67 and caspase was conducted to assess proliferative activity and apoptosis, respectively. Mitotic activity was assessed by counting mitotic figures in ten high powered (400×) fields. Ki67 labeling indices were assessed semiquantitatively.

Statistical analysis

For the nonimaging study, the differences among the different concentrations of ficlatuzumab and the different chemotherapy agents were evaluated using a log-rank test with Bonferroni corrections.

For the initial (first) imaging experiment, the relative efficacy of FDG PET to FLT PET was assessed by correlating the respective PET signal (ratio of maximal tumor to normal brain activity) to the comparative bioluminescence signal as well as to each other. The Student *t* test was used to assess significance of the latter comparison.

In the follow-up (second) imaging experiment, single-factor ANOVA was used to evaluate the relative efficacy of each imaging modality in assessing tumor response to the novel chemotherapeutic agent. Tukey *post hoc* pairwise comparisons were done as needed to assess significance of the differences among the 4 imaging time points.

The quantitative assessment of mitotic activity from all three groups was analyzed with ANOVA and unpaired *t* tests. In all cases, a cutoff value of $P < 0.05$ was used to assess statistical significance.

Results

Dose titration of ficlatuzumab

A dose-dependent improvement in survival benefit is evident in mice treated with ficlatuzumab compared to 10 mg/kg human IgG1 isotype control. While the median survival time for isotype-treated animals was 20 days ($n = 10$), the median survival time for all three groups of ficlatuzumab-treated animals were significantly higher ($P < 0.0001$) than the isotype control group (Supplementary Fig. S1). Comparing the three doses (5, 10, and 20 mg/kg) of ficlatuzumab, there was no significant difference between the 5 and 10 mg/kg doses ($P = 0.5205$) or 10 and 20 mg/kg doses ($P = 0.2521$) but there was between the 5 and 20 mg/kg doses ($P = 0.0137$). A fixed dose of 10 mg/kg of ficlatuzumab was used in combination with temozolomide in a follow-up study described next.

Combination therapy of ficlatuzumab and temozolomide studied in an intracranial U87 MG xenograft mouse model

The intermediate effective dose for ficlatuzumab (10 mg/kg) and temozolomide (5 mg/kg) were selected for a follow-up study to evaluate the antitumor effect of these agents. During

the study, one of the mice in 10 mg/kg ficlatuzumab treatment group had a palpable skin outgrowth that was determined to be unrelated to study manipulations and was excluded from analyses. As seen in Supplementary Fig. S2, a concurrent combination therapy of 5 mg/kg temozolomide with 10 mg/kg ficlatuzumab significantly increased the survival benefit compared to either single-agent therapy in mice bearing intracranial U87 MG tumors. While 8 of 10 mice (80%) remained free of any clinical signs of disease after stopping treatment in the combination therapy arm, only 1 of 9 mice (11%) survived with the 10 mg/kg ficlatuzumab monotherapy. No mice survived treatment with isotype IgG1 or 5 mg/kg temozolomide.

Creation and confirmation of U87 MG-Luc 2 stable cell line

U87 MG (HTB-14 from ATCC) was stably transfected with a firefly luciferase construct as described in the Methods. The clonal cell line U87 MG-Luc2 was evaluated for its growth, morphology, and *in vivo* tumorigenicity in side-by-side comparison with the parental cell line and found to be similar in its properties to U-87 MG (Supplementary Fig. S3). This clone was estimated to show a bioluminescence signal equivalent to 1250 photons/sec/cell *in vitro* under experimental conditions tested, and the signal was found to be stable over a period of 5 weeks in culture.

Evaluation of FDG versus FLT small-animal PET for the evaluation of orthotopic brain tumor model

All mice survived the surgeries and tolerated the procedure without any observable negative effects. There was a steady increase in the BLI signal over the course of 5 weeks (Table 1). Both visually and quantitatively, FLT PET provided a better signal-to-background ratio than FDG PET within the brain ($P = 0.01$; Fig. 1). The FLT signal was appreciable when the BLI signal reached approximately 3×10^7 p/s/cm^2/sr, which occurred approximately 4 weeks postimplantation. The FDG signal never increased significantly above background levels in the brain.

Comparison of BLI, small-animal FLT PET, and small-animal MRI for the *in vivo* evaluation of tumor response to ficlatuzumab

All mice survived the surgeries and tolerated the procedure without any observable negative effects. The weight of the mice did not significantly change over the course of the experiment in any of the experimental groups (Supplementary Fig. S4). Representative images from each of the imaging modalities are shown in Fig. 2. The pathology specimens showing the H&E, Ki-67, and caspase stains are shown in Fig. 3.

Of note, for all the imaging modalities, the baseline (starting) values for the drug groups are higher than for the control group. This is likely because the baseline imaging for those groups was started 3 days later than for the control group.

In the control group, there was steady tumor progression in terms of cell viability (BLI), metabolism (PET), and size (MRI) over the 2 weeks of the experiment. The results were in accord between the BLI, PET, and MRI (Fig. 4, Table 2, Supplementary Table S1), although most pronounced with the modalities of BLI and PET. In all cases, the measured parameters

(i.e., photon flux, FLT uptake, and tumor volume, respectively) were significantly different across the 4 experimental time points.

In the low-dose group, there was a marked decline in the tumor based on cell viability and metabolically, but not anatomically (Fig. 4, Table 2, Supplementary Table S1). For both BLI and PET, the differences across the 4 experimental time points were significantly different, with a marked drop in photon flux or PET uptake (mean and max) after the first drug injection was given, then remaining low throughout the remainder of the experiment. For MRI, there was an initial increase in tumor volume after the first injection, which then returned to baseline levels after the 2nd injection, and further dropped after the 3rd injection. These changes were not statistically significant.

The results of the high-dose group mirrored that of the low-dose group. Again, the cell viability and metabolic modalities showed a steady decline in tumor activity whereas MRI did not (Fig. 4, Table 2, Supplementary Table S1). The BLI data again showed significant differences across the time points with a marked drop in photon flux after the first injection, then remaining low throughout the remainder of the experiment. The PET data showed a similar trend, although the results were not significant, likely because of a high SD. Finally, the MRI data again showed an initial increase in size after the 1st injection, which remained stable after the 2nd injection, and then markedly dropped (below baseline) after the 3rd drug injection. These changes were not statistically significant.

Pathology—Mitotic activity was assessed in each of the animals in the most proliferative areas of tumor (Supplementary Table S2). The mitotic activity was highest in the control group with a mean ± SD of 56 ± 8.5 mitotic figures per 10 high-powered fields (HPF), with diminished mitotic activity in the low-dose and high-dose groups, respectively (low-dose: 47 ± 11.8, and high-dose: 15.7 ± 8.1). One-way ANOVA analysis shows a significant difference in the mitotic activity among the three groups ($P < 0.001$). *T* tests comparing individual groups show significant differences between the low-dose and high-dose groups ($P < 0.05$), as well as between the control group and the high-dose groups ($P < 0.01$). The mitotic counts also correlated with the Ki-67 labeling indices, which showed the highest percentage of nuclear labeling in the control group, with decreased activity in the low-dose and high-dose groups. Nuclear caspase activity was present in all three groups and showed no significant difference among the three groups.

Discussion

Gliomas, while rare, are of medical importance given the very poor outcomes with currently therapies. Ficlatuzumab is a novel anti-HGF/c-MET antibody current in phase II development. This article summarizes the background pre-clinical work conducted on ficlatuzumab. This includes evaluation of the dose response to ficlatuzumab, a comparison to the current standard of care, temozolomide, followed by noninvasive evaluation of response to therapy using various small-animal imaging modalities focusing on those modalities that have the potential to be used clinically.

c-MET is a proto-oncogene that encodes for the protein hepatocyte growth factor receptor (HGFR) and functions as a receptor tyrosine kinase. HGF is the only known ligand of the MET receptor. Upon HGF stimulation, c-MET induces several biologic responses in cancer cells including promotion of tumor growth, angiogenesis, and metastasis. Deregulation of this pathway has been implicated in many tumors including bladder, lung, breast, gastric, ovarian, prostate, colorectal, head and neck, certain sarcomas and several other solid tumors as well as hematologic malignancies. The traditional chemotherapy agent used in this study, temozolomide, is an oral alkylating agent. Its therapeutic benefit arises from the alkylation or methylation of DNA, which subsequently causes tumor cell death. It is primarily used for gliomas. The newer compound, ficlatuzumab, is a humanized monoclonal antibody that specifically targets the anti-HGF/c-MET pathway and is thought to block the aforementioned programmed invasive growth. As such, it would in theory be effective against the variety of cancers that c-MET has been implicated in.

In this study, the focus was on a mouse brain orthotopic model using U87 MG cells. The dose response to ficlatuzumab was established first using survival times as an endpoint. Significantly longer survival times with ficlatuzumab were seen in comparison to control, and a dose of 10 mg/kg was established for further studies. Next, survival times were compared for ficlatuzumab against the current standard of care, temozolomide. Both ficlatuzumab and temozolomide provided a survival advantage over control animals, but the greatest survival was seen with a combined therapy strategy using both drugs.

The goal of the next phase of the study was to evaluate the ability to noninvasively assess response to ficlatuzumab in this mouse brain orthotopic model. There has already been a fair amount of literature on this subject for small animals with brain tumors. An early study by Kim and colleagues (5) used T2-weighted spin-echo MRI sequences to evaluate the growth curve of intracranially placed 9L brain tumors in rats, finding an exponential growth curve over the lifespan of the animal. Others have successfully used dynamic contrast–enhanced MR sequences to evaluate angiogenesis and the response to anti-angiogenic therapy (6, 7). van Furth and colleagues (8) used a clinical 1.5T MR system to image murine brain tumors with the application of a specially designed surface coil.

Some work has also been done with different radiopharmaceuticals and small animal PET imaging. Jost and colleagues (9) compared treatment response of intracranial glioblastoma tumors in mice using 3 different radiotracers including FDG, FLT, and 11C-RHM-1 (a sigma2-receptor ligand for proliferation) as well as 4.7T MRI and optical imaging. They found significant correlation among BLI, PET, and MRI in their study, although only tumor growth (not treatment response) was being evaluated. Swanson and colleagues (10) compared T1- and T2-weighted MRI sequences with ^{18}F-fluoromisonidazole (FMISO) PET to evaluate for hypoxia. In this case, the MRI and PET provided complementary but distinct information about the intracranial glioblastoma tumors.

The two imaging modalities chosen in the current experiment were PET and MRI as they are not only both used clinically but are also available for small-animal imaging. To additionally directly assess cell viability in the mice, BLI was used for comparison. Cell culture and *in*

vivo survival studies did not show any differences between the original U87 MG cells and the new U87 MG-Luc2 cells.

While FDG PET is the current standard of care for the majority of human clinical oncologic imaging, many other radiopharmaceuticals are available with different biodistribution and kinetics. One such radiotracer, FLT, is particularly promising for brain imaging given its very low background uptake in normal brain. As such, both radiotracers were initially imaged in a preliminary study to establish the relative use of FDG versus FLT PET imaging in this mouse brain orthotopic model. The findings showed that BLI is more sensitive than small-animal PET, yielding a detectable tumor signal weeks earlier. Second, the FLT signal is seen when the BLI signal greater than or equal to approximately 3×10^7 p/s/cm^2/sr, providing a tumor-to-brain ratio of approximately 3. The FDG signal, however, never rose above a tumor-to-brain ratio of 1. As such, the FLT provides a better signal-to-background ratio than FDG and was chosen for the subsequent phase of this study.

The final phase of this study compared the relative efficacy of BLI, FLT PET, and MRI to evaluate noninvasive response to ficlatuzumab in the mouse brain orthotopic model. In this experiment, two different doses of ficlatuzumab, in addition to a control group, were used to determine whether dose response could also be assessed non-invasively. The results show that, first, BLI again appears to have the greatest sensitivity for small changes and was significantly different in all 3 experiment groups: control, low dose, and high dose.

FLT PET also conducted quite well with regard to response assessment and showed significant changes in the control and low-dose groups, with the same findings as for BLI. In the high-dose group, the trend of the changes was also the same, but the findings did not reach statistical significance because of higher variability in the data. The latter would likely be overcome with the use of a larger sample size.

MRI showed the most variability. On one hand, as shown in the images, the ability to assess volumes and directly visualize a relatively small (several millimeters in diameter) tumor in mouse brain is quite good and clearly better than BLI or PET. Evaluation of surrounding edema and mass effect (tumor causing displacement of adjacent normal structures) is also possible. However, aside from the control group, the changes seen with MRI were not statistically significant. Specifically, it did not show a significant change in tumor volume with either the low-dose or high-dose drug injection. Interestingly, both drug groups showed an initial increase in tumor volume, followed by a decrease after the 2nd injection (low-dose group) or 3rd injection (high-dose group). The reason for this pattern is unclear, although various hypotheses can be proposed. FLT, as it measures DNA synthesis and is an indirect marker of proliferation, is really imaging rate of growth, and if the cytostatic effects of ficlatuzumab outweigh the cytotoxic effects, that might explain the continued growth seen on MRI, despite a decrease in metabolic tumor burden. However, the decrease in viable cell signal (BLI) even after the first drug injection argues against this. Alternatively, the enlargement seen on MRI may be due to surrounding edema rather than true tumor growth. Gadolinium contrast was not used for these MRI scans such that differentiating tumor from surrounding edema is limited.

Quantitative assessment of mitotic activity in the three groups showed statistically significant differences in proliferative activity between the control and treatment groups in terms of both absolute mitotic activity and Ki-67 labeling indices. This difference in proliferative activity was most marked between the control and high-dose groups. We nonetheless interpreted these results with caution given the small sample size. These findings are in line with the results of BLI and PET and less supportive of the MRI findings. Overall, the results of the current study support the translation of FLT PET to human clinical trials evaluating the response to novel therapies of glioblastoma.

There are several limitations of the current study. First, the sample size is small relative to the variation across individual mice, making it difficult to achieve statistical significance in some cases. Another limitation is that mice form small tumors and even with the use of a dedicated small animal imaging apparatus, results in volume averaging artifacts. As partial volume corrections were not done, the PET activity was likely underestimated when the tumor dimensions are less than twice the full-width half-maximum spatial resolution of the scanner. Nonetheless, the PET results were consistent with the BLI and histopathologic result, suggesting they are robust. As mentioned, the MRI data were collected without the use of gadolinium contrast. Its use may have helped differentiate between the true margins of the tumor and surrounding edema or unrelated and nonspecific findings. Similarly, the use of only one pulse sequence may have limited fuller evaluation of the tumor. Certainly, the limitations mentioned thus far can form the foundation of a follow-up experiment to confirm the findings. Finally, the baseline values for the drug groups were higher than those of the control group. While not ideal, as mentioned, this is likely a reflection of the fact that imaging on those groups was started a few days later than the imaging for the control group. However, by evaluating Supplementary Table S1 in which the percent change is shown rather than the absolute change, it can be seen that the percent change shows the same effects as the absolute changes. As such, this difference is unlikely to have had a major effect on the overall results.

Supplementary Material

Refer to Web version on PubMed Central for supplementary material.

Acknowledgments

The authors thank Dr. Satya Medicherla for discussions and input on the study design, and Dr. Fred Chin and his radiochemistry team for production of FDG and FLT.

Grant Support

The authors thank funding support from the Ben and Catherine Ivy Foundation and from National Cancer Institute (NCI) In Vivo Cellular and Molecular Imaging Center (ICMIC) P50 CA114747 (to S.S. Gambhir).

References

1. Howlader, N.; Noone, AM.; Krapcho, M.; Neyman, N.; Aminou, R.; Waldron, W., et al. SEER cancer statistics review, 1975–2008. Bethesda, MD: National Cancer Institute; 2008.
2. Schneider T, Mawrin C, Scherlach C, Skalej M, Firsching R. Gliomas in adults. Dtsch Arztebl Int. 2010; 107:799–807. [PubMed: 21124703]

3. Patnaik A, Weiss GJ, Papadopoulos K, Tibes R, Tolcher AW, Payumo FC, et al. Phase I study of SCH 900105 (SC), an anti-hepatocyte growth factor (HGF) monoclonal antibody (MAb), as a single agent and in combination with erlotinib (E) in patients (pts) with advanced solid tumors. J Clin Oncol. 2010; 28(suppl):15s. abstr 2525.

4. Tan E, Park K, Lim WT, Ahn M, Ng QS, Ahn JS, et al. Phase Ib study of ficlatuzumab (formerly AV-299), an anti-hepatocyte growth factor (HGF) monoclonal antibody (MAb) in combination with gefitinib (G) in Asian patients (pts) with NSCLC. J Clin Oncol. 2011; 29(suppl):abstr 7571.

5. Kim B, Chenevert TL, Ross BD. Growth kinetics and treatment response of the intracerebral rat 9L brain tumor model: a quantitative *in vivo* study using magnetic resonance imaging. Clin Cancer Res. 1995; 1:643–50. [PubMed: 9816027]

6. Gossmann A, Helbich TH, Kuriyama N, Ostrowitzki S, Roberts TP, Shames DM, et al. Dynamic contrast-enhanced magnetic resonance imaging as a surrogate marker of tumor response to anti-angiogenic therapy in a xenograft model of glioblastoma multiforme. J Magn Reson Imaging. 2002; 15:233–40. [PubMed: 11891967]

7. Veeravagu A, Hou LC, Hsu AR, Cai W, Greve JM, Chen X, et al. The temporal correlation of dynamic contrast-enhanced magnetic resonance imaging with tumor angiogenesis in a murine glioblastoma model. Neurol Res. 2008; 30:952–9. [PubMed: 18662497]

8. van Furth WR, Laughlin S, Taylor MD, Salhia B, Mainprize T, Henkelman M, et al. Imaging of murine brain tumors using a 1. 5 Tesla clinical MRI system. Can J Neurol Sci. 2003; 30:326–32. [PubMed: 14672264]

9. Jost SC, Wanebo JE, Song SK, Chicoine MR, Rich KM, Woolsey TA, et al. In vivo imaging in a murine model of glioblastoma. Neurosurgery. 2007; 60:360–70. [PubMed: 17290188]

10. Swanson KR, Chakraborty G, Wang CH, Rockne R, Harpold HL, Muzi M, et al. Complementary but distinct roles for MRI and 18F-fluoromisonidazole PET in the assessment of human glioblastomas. J Nucl Med. 2009; 50:36–44. [PubMed: 19091885]

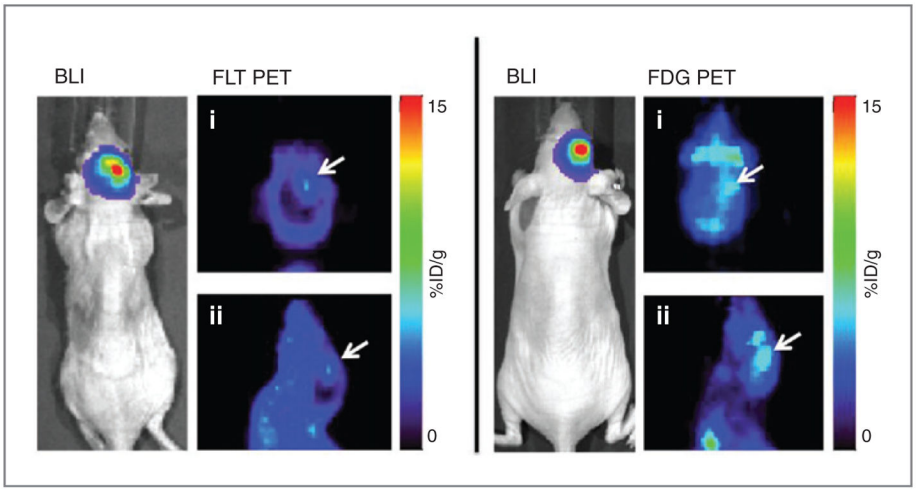

Figure 1.

Whole-body BLI and small-animal PET images of the head [coronal (i); sagittal (ii)] showing tumor (white arrows) visibility at 4 weeks post-tumor cell implantation. Both mice shown have similar luminescence of 4×10^7 p/s/cm^2/sr. The FLT signal is greater than that of brain background, whereas the FDG signal is not.

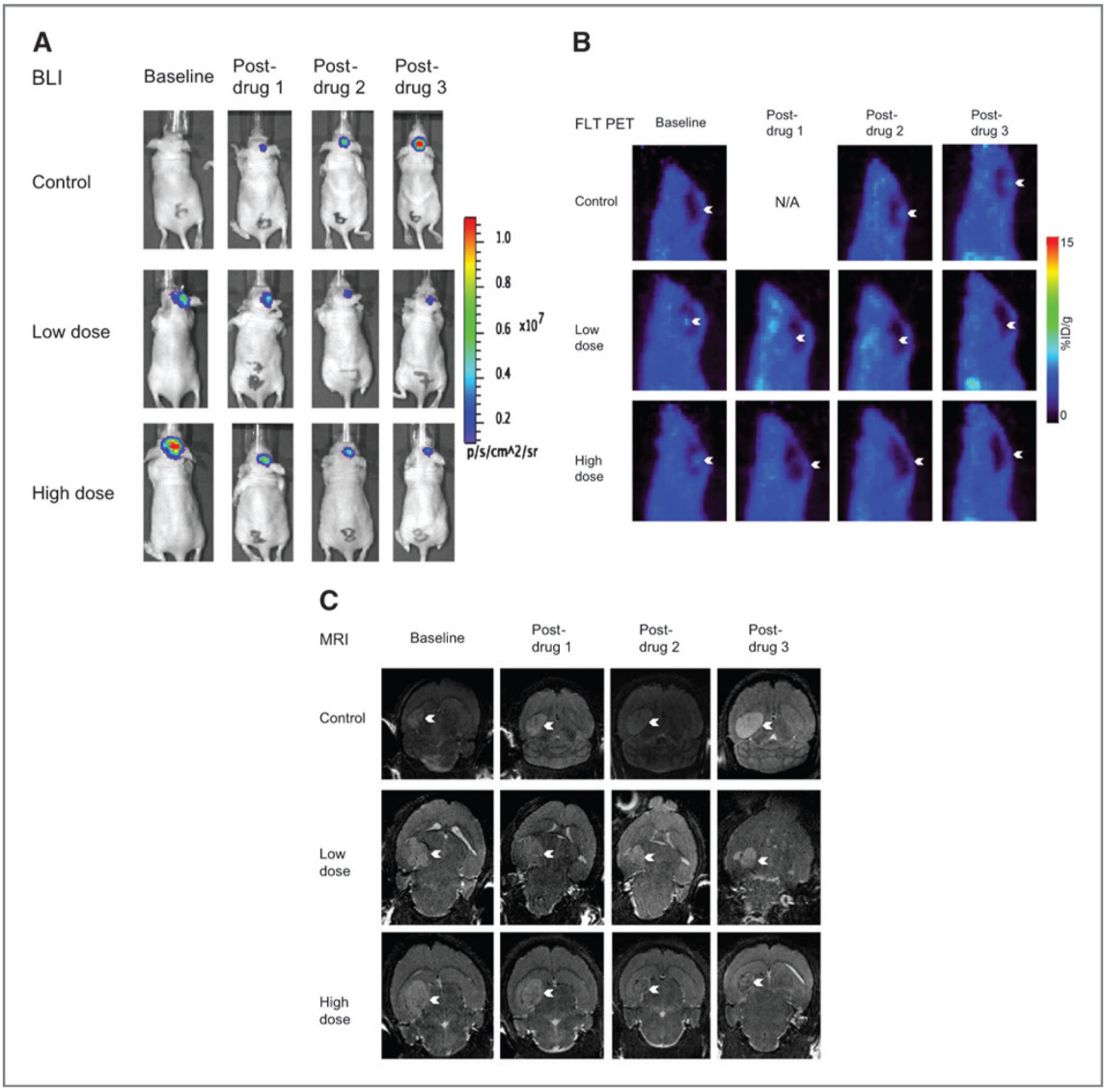

Figure 2.

Representative imaging of BLI (A), FLT PET (B), and MRI (C). For each group of images, the same mouse is shown from each of the 3 groups: control, low-dose, and high-dose (*x*-axis). Also for each group of images, each animal is shown at baseline, post-drug 1, post-drug 2, and post-drug 3 (*y*-axis).

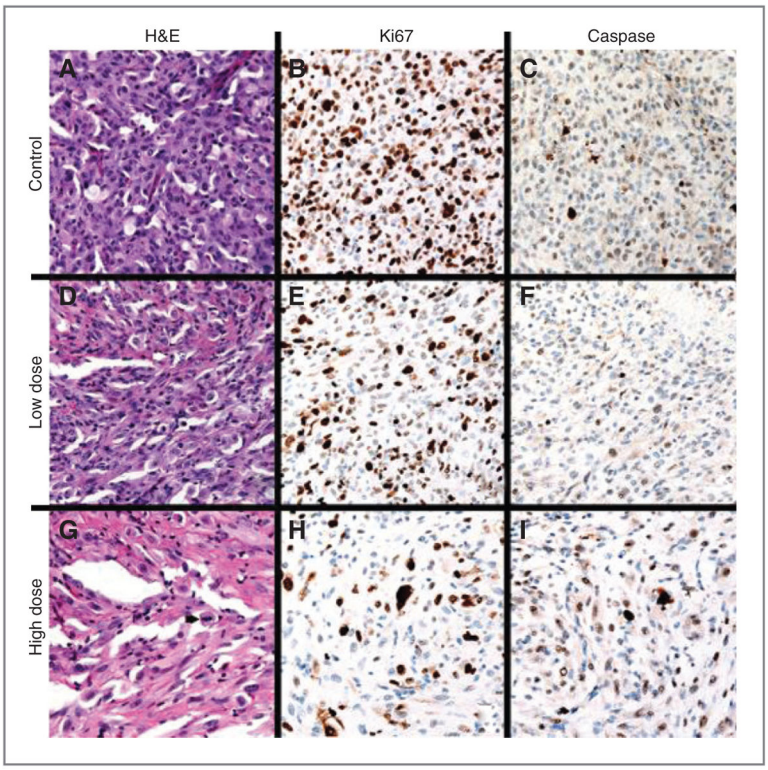

Figure 3.

A–C, (top row, left to right) Control animal 1, H&E 400× (A) with 3 mitotic figures (white arrowheads) in a single HPF; Ki-67 400× (B) labeling approximately 80% of tumor cell nuclei; caspase 400× (C) labeling a subset of tumor cell nuclei. D–F, (second row, left to right) low-dose animal 3, H&E 400× (D) with one mitotic figure (white arrowhead) in a single HPF; Ki-67 400× (E) labeling approximately 50% of tumor cell nuclei; caspase 400× (F) labels rare tumor cell nuclei. G–I, (third row, left to right) high-dose animal 2, H&E 400× (G) with one mitotic figure (black arrowhead) in a single HPF; Ki-67 400× (H) labeling approximately 20% of tumor cell nuclei; caspase 400× (I) labeling a subset of tumor cell nuclei.

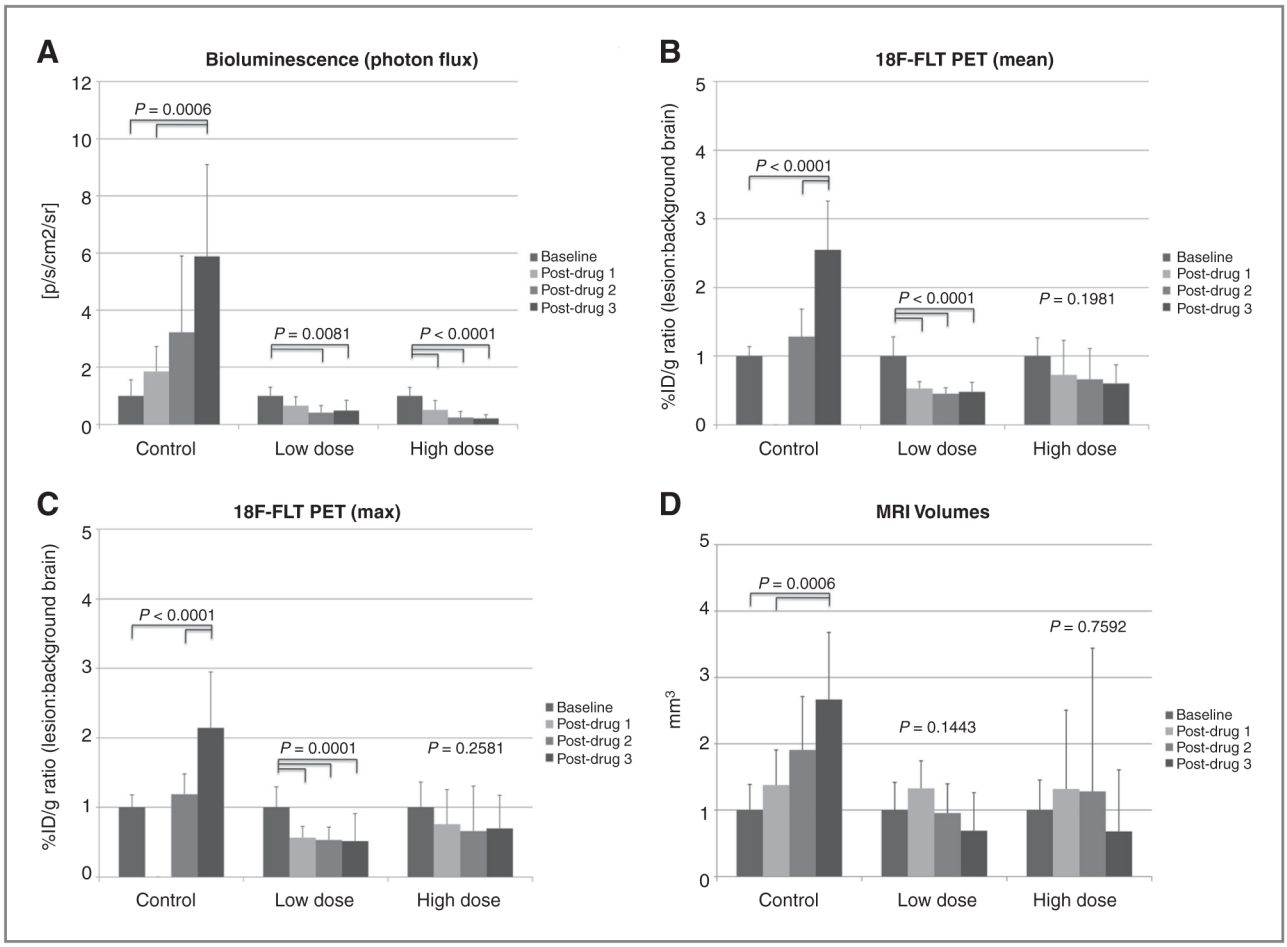

Figure 4.

A, change in tumor bioluminescence signal (a), mean FLT PET signal (b), maximum FLT PET signal (c), and volume (d) (mean ± SD) over the course of the experiment in the control, low-dose, and high-dose groups. The values and error bars represent the mean and SD, respectively. Results shown are normalized to their respective baseline value. The *P* values shown are the results of the ANOVA for each group. For those groups with significant differences, the significantly different pairs are indicated. B, change in mean PET signal (mean ± SD) over the course of the experiment in the control, low-dose, and high-dose groups. Results shown are normalized to the baseline value. The *P* values shown are the results of the ANOVA for each group. For those groups with significant differences, the significantly different pairs are highlighted. C, change in maximum PET signal (mean ± SD) over the course of the experiment in the control, low-dose, and high-dose groups. Results shown are normalized to the baseline value. The *P* values shown are the results of the ANOVA for each group. For those groups with significant differences, the significantly different pairs are highlighted. D, change in tumor volumes as measured by MRI over the course of the experiment in the control, low-dose, and high-dose groups. The *P* values shown are the results of the ANOVA for each group. For those groups with significant differences, the significantly different pairs are highlighted.

Table 1

Average and standard deviation (SD) of bioluminescence, FLT PET, and FDG PET signals in untreated tumor-bearing mice over 5 weeks post-tumor cell implantation

	Bioluminescence (p/s/cm^2/sr)		Tumor: normal brain ratio of FLT		Tumor: normal brain ratio of FDG	
	Average	SD	Average	SD	Average	SD
Week 1	1.52E ± 06	2.24E ± 06	1.3	0.9	0.9	0.8
Week 2	2.62E ± 06	3.68E ± 06	1.8	2.3	0.9	0.9
Week 3	4.96E ± 06	5.83E ± 06	1.9	2.2	0.9	0.8
Week 4	3.02E ± 07	3.25E ± 07	2.6	2.1	0.9	0.8
Week 5	4.99E ± 07	6.98E ± 07	1.8	4.0	1.1	1.5

Clin Cancer Res. Author manuscript; available in PMC 2016 April 09.

Table 2

Overall results of second experiment shown as actual values by experimental group: control, low dose, and high dose

Average	Weight, g	Bioluminescence, p/s/cm^2/sr	PET mean, %ID/g ratio	PET max, %ID/g ratio	MRI, mm^3
Control					
Baseline	22.8	7.40E ± 05	1.00	1.14	5.02
Post-drug 1	22.2	1.37E ± 06	—	—	6.92
Post-drug 2	21.3	2.39E ± 06	1.28	1.35	9.57
Post-drug 3	22.1	4.36E ± 06	2.55	2.44	13.37
SD					
Baseline	1.9	4.18E ± 05	0.1	0.2	1.9
Post-drug 1	1.8	6.46E ± 05	—	—	2.7
Post-drug 2	2.6	1.98E ± 06	0.4	0.3	4.0
Post-drug 3	2.1	2.38E ± 06	0.7	0.8	5.1
ANOVA	0.5628	0.0006	<0.0001	<0.0001	0.0006
		Bv3, 1v3	Bv3, 2v3	Bv3, 2v3	Bv3, 1v3
Low dose					
Baseline	22.7	1.39E ± 06	3.22	2.58	20.43
Post-drug 1	22.6	9.11E ± 05	1.70	1.46	27.09
Post-drug 2	22.1	5.75E ± 05	1.46	1.38	19.46
Post-drug 3	21.7	6.76E ± 05	1.55	1.34	14.10
SD					
Baseline	1.7	4.29E ± 05	0.9	0.8	8.6
Post-drug 1	2.0	4.39E ± 05	0.3	0.40	8.5
Post-drug 2	2.2	3.46E ± 05	0.3	0.2	9.1
Post-drug 3	2.4	5.05E ± 05	0.5	0.4	11.7
ANOVA	0.8136	0.0081	<0.0001	0.0001	0.1443
		Bv2, 3	Bv1, 2, 3	Bv1, 2, 3	
High dose					
Baseline	23.7	2.11E ± 06	2.55	2.10	15.86
Post-drug 1	24.0	1.07E ± 06	1.85	1.59	20.92
Post-drug 2	23.3	5.11E ± 05	1.69	1.39	20.32

Average	Weight, g	Bioluminescence, p/s/cm^2/sr	PET mean, %ID/g ratio	PET max, %ID/g ratio	MRI, mm^3
Post-drug 3	24.2	4.42E ± 05	1.53	1.47	10.80
SD					
Baseline	0.9	6.32E ± 05	0.7	0.8	7.2
Post-drug 1	0.9	7.03E ± 05	1.3	1.1	18.8
Post-drug 2	0.7	4.53E ± 05	1.1	0.6	34.2
Post-drug 3	1.0	2.81E ± 05	0.7	0.5	14.7
ANOVA	0.1787	<0.0001	0.1981	0.2581	0.7592
		Bv1, 2, 3			